Invest New Drugs (2018) 36:370–379
https://doi.org/10.1007/s10637-017-0538-9

PRECLINICAL STUDIES

Cyclodextrin polymers as nanocarriers for sorafenib

Valentina Giglio[1] · **Maurizio Viale**[2] · **Vittorio Bertone**[3] · **Irena Maric**[2] · **Rita Vaccarone**[3] · **Graziella Vecchio**[1]

Received: 30 August 2017 / Accepted: 31 October 2017 / Published online: 8 November 2017

Summary Polymeric nanoparticles based on cyclodextrins are currently undergoing clinical trials as new promising nanotherapeutics. In light of this interest, we investigated cyclodextrin cross-linked polymers with different lengths as carriers for the poorly water-soluble drug sorafenib. Both polymers significantly enhanced sorafenib solubility, with shorter polymers showing the most effective solubilizing effect. Inclusion complexes between sorafenib and the investigated polymers exhibited an antiproliferative effect in tumor cells similar to that of free sorafenib. Polymer/Sorafenib complexes also showed lower in vivo tissue toxicity than with free sorafenib in all organs. Our results suggest that the inclusion of sorafenib in polymers represents a successful strategy for a new formulation of this drug.

Keywords Anticancer drug · Drug carriers · Nanoparticles · Solubility · Toxicity

Introduction

Cyclodextrins (CyDs) are cyclic oligosaccharides consisting of α-1,4-linked glucopyranose units with a hydrophilic outer surface and a hydrophobic central cavity. CyDs are widely used as pharmaceutical excipients, enhancing chemical stability and improving the shelf-lives of drugs [1]. Several chemical functionalizations are possible on CyDs to improve their properties in pharmaceutical and biomedical applications [2–10]. An example of an important CyD derivative is sugammadex, which is based on γ-CyD. Sugammadex acts as a selective binding agent that encapsulates the muscle relaxant rocuronium, considerably shortening the recovery time of muscular tone in patients after general anesthesia [11]. The use of CyDs in the formulation of poorly water-soluble drugs is of particular interest [12]. CyDs can, in fact, increase the apparent solubility of many drugs, thus increasing their bioavailability and allowing for them to reach systemic circulation or the desired target site [13].

More recently, the synthesis of stable CyD nanoparticles (NPs) [14] has attracted considerable interest, and a variety of organic and hybrid CyD-based NPs have been synthesised [15–19]. The cyclosert delivery platform, for instance, is a successful example of linear CyD polymers designed as drug nanocarriers [20–22]. Many CyD-based polymers have been prepared by linking CyD units with crosslinkers (i.e. cross-linked polymers). Epichlorohydrin (EPI) has also been used as a crosslinker, and EPI cross-linked polymers have been widely investigated as drug nanocarriers [23–25]. Typically, CyD polymers exhibit a greater drug-carrying capacity than simple CyDs [26–28]. More recently, oligomers of CyDs have also been studied as drug carriers [6, 26]. One potential advantage of oligomers of CyDs is that they are easier to excrete through the renal tubules without degradation [29]. On this basis, we investigated EPI-crosslinked CyD nanocarriers to tackle the low-solubility of sorafenib (Nexavar, SFN).

SFN is an oral multikinase inhibitor approved by the U.S. Food and Drug Administration in 2006 for the treatment of patients with advanced renal cell carcinoma or unresectable hepatocellular carcinoma. SFN displays

✉ Graziella Vecchio
gr.vecchio@unict.it

[1] Dipartimento di Scienze Chimiche, Università degli Studi di Catania, V.le A.Doria 6, 95125 Catania, Italy

[2] Ospedale Policlinico San Martino, U.O.C. Bioterapie, L.go R. Benzi, 10, 16132 Genova, Italy

[3] Dipartimento Biologia e Biotecnologie, Lab. Anatomia Comparata e Citologia "L. Spallanzani", Università di Pavia, Via Ferrata 9, 27100 Pavia, Italy

antitumor activity across a variety of tumor types, including renal, hepatocellular, breast, thyroid and colorectal carcinomas. SFN also inhibits several tyrosine kinase receptors involved in tumor progression and tumor angiogenesis [30]. According to the biopharmaceutical classification system (BCS), in vitro studies catalog SFN as a class II drug [31]. In fact, SFN is water soluble at a rate of 9.86 ng/mL in a neutral pH environment [32], and its oral bioavailability is low (about 8.5%, oral administration), due to its low aqueous solubility [33]. SFN tosylate is used as tablets (Nexavar, Bayer Healthcare Pharmaceuticals–Onyx Pharmaceuticals) to slightly improve its solubility. Some formulations have been prepared to increase the solubility and bioavailability of SFN [34, 35]. Despite its inherent selectivity, SFN can cause unusual adverse reactions, including severe respiratory and liver failure, thus posing a challenge for oncologists [36–39].

In particular, we prepared the inclusion complexes of a β-CyD polymer (92 kDa) and oligomer (12 kDa) with SFN (Fig. 1). We determined the complexation efficiency (CE) of the hosts and tested the cytotoxicity of the inclusion complexes and SFN in different cell lines. We also determined the in vivo tissue toxicity of SFN and its soluble complexes.

Materials and methods

Chemicals

All chemicals obtained from commercial sources were used without further purification. The water-soluble polymer pCyD (92 kDa, 70% of CyDs, 57 CyD units) was purchased from CyClolab. CyD oligomer (oCyD, 12 kDa, 65% of CyD, 7 CyD units) was synthesised as described elsewhere [40].

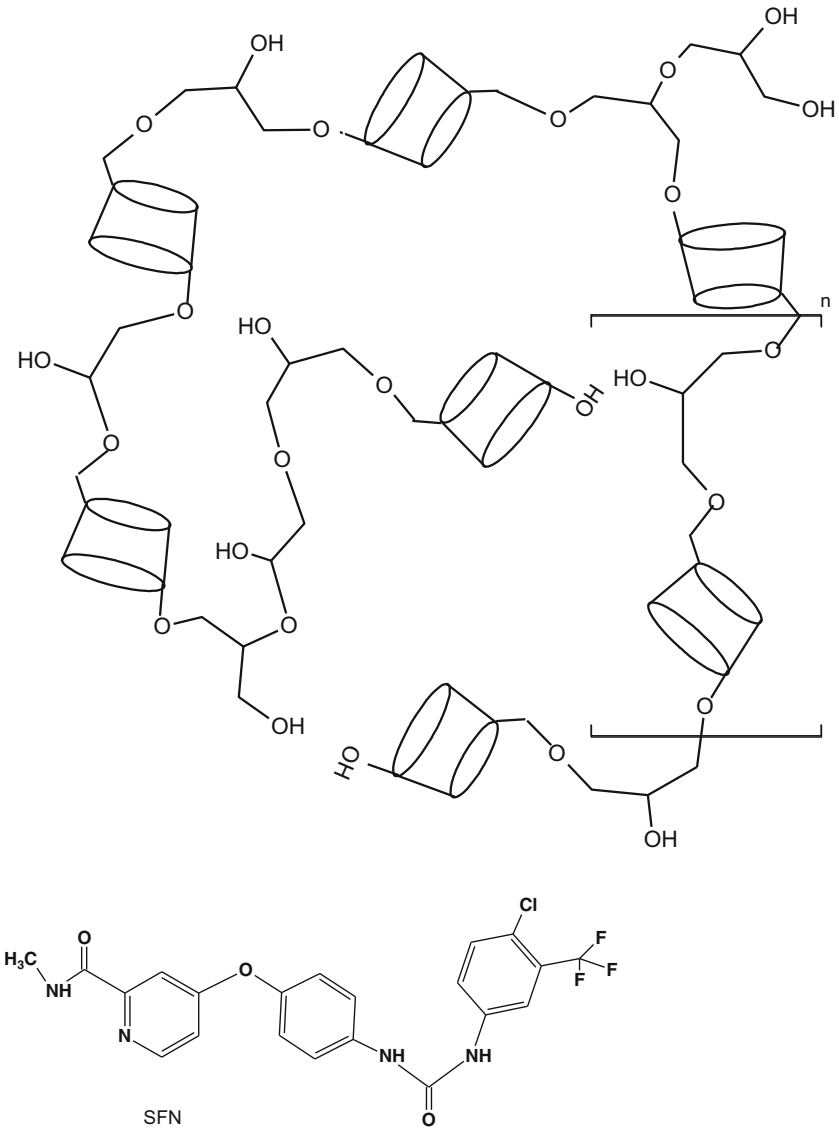

Fig. 1 Schematic structure of cross-linked polymers ($n \approx 1$ oCyD & $n \approx 50$ pCyD) and sorafenib (SFN)

oCyD: Dimension (DLS): 3.8 ± 0.8 nm. Zeta potential: 2.1 ± 1 mV.

NMR spectroscopy

^{1}H NMR spectra were recorded at 25 °C with a Varian UNITY PLUS-500 spectrometer at 499.9. NMR spectra were recorded by using standard pulse programmes from the Varian library.

Light scattering measurements

Dynamic light scattering (DLS) measurements were performed at 25 °C with a Zetasizer Nano ZS (Malvern Instruments, UK) operating at 633 nm (He–Ne laser).

UV/Vis and circular dichroism spectroscopy

UV/Vis spectra were recorded using an Agilent 8452A diode array spectrophotometer. CD spectra were recorded with a JASCO J-1500 spectropolarimeter at 25 °C.

Solubility studies

Phase-solubility studies were performed in aqueous solutions. An amount of SFN (7 mg) was added to 2 mL aqueous solutions containing different concentrations of β-CyD, oCyD or pCyD in Tris (tris(hydroxymethyl)aminomethane) buffer (10 mM, pH 7.4).

After an incubation time of 12 h at 25 °C, the suspension was centrifugated, and SFN concentration was determined in the supernatant by UV/Vis spectroscopy at 268 nm. A plot of the solubility of SFN (S_{SFN}) versus the total concentration of CyD cavities ([CyD]t) was obtained. The A_L-type diagrams fitted with the following eq. [41]:

$$S_{SFN} = So_{SFN} + K_{1:1}So/(1 + K_{1:1}So)[CyD]t$$

CE was calculated from the slope of the straight line obtained:

$$CE = So_{SFN}K_{1:1} = Slope/(1-Slope)$$

The apparent stability constant $K_{1:1} = CE/S_0$ was calculated for S_0 = the intrinsic solubility of SFN. Calibration curves of SFN in the presence of CyD polymers were used to determine S_{SFN} values. The molar absorptivity of SFN, determined in an aqueous solution of pCyD or oCyD, was 45,300 (mol^{-1} L cm^{-1}) and 47,000 (mol^{-1} L cm^{-1}), respectively.

CyD polymer/SFN complexes for biological assays

Solutions for the in vitro study were prepared by adding 50 μL of a DMSO solution of SFN (10 mg/mL) to a solution (2 mL) of pCyD or oCyD (10 mg/mL, Milli-Q water). Solutions for the in vivo toxicity study were prepared by adding 100 μL of a DMSO solution of SFN (200 mg/mL) to a solution (10 mL) of pCyD or oCyD (50 mg/mL). The solutions were stirred for 8 h and then filtered. The final concentration of SFN was determined using UV-Vis spectroscopy.

Cell cultures

Human breast carcinoma MCF-7, gastric carcinoma HGC-27, liver cancer HepG2 and melanoma SKMel-28 cells were grown in DMEM medium (Euroclone, Pero, Italy) supplemented with 10% FBS and 1% penicillin-streptomycin (Euroclone). Tumor thyroid K1 cells were grown in DMEM medium/F12 medium (1:1), supplemented with 10% FBS and 1% penicillin-streptomycin.

3-(4,5-dimethylthiazol-2-yl)-2,5-diphenyltetrazolium bromide (MTT) assay

Cell lines were plated into flat-bottomed, 96 well microtiter plates at appropriate concentrations. After a 6–8 h incubation, cells were treated with solutions of SFN or the selected SFN complexes (five concentrations). After a 72 h treatment, the MTT assay was used as described elsewhere [42]. The IC_{50} values were calculated from the analysis of single concentration-response curves; each final value is the mean of 4–7 experiments.

Apoptosis by 4,6-diamidino-2-phenylindole (DAPI) staining

MCF-7, K1, HepG2 and HGC-27 cells were plated in 1 mL at opportune densities/well into 24 well-microtiter plates. After about 6–8 h, SFN, pCyD/SFN and oCyD/SFN were added at their IC_{50} and IC_{75} values. All floating and adherent cells were harvested 3 d later, washed with a saline solution and fixed with 100 μl of 75% ethanol in phosphate-buffered saline. For the microscope analysis, samples were treated with 6 μL of DAPI aqueous solution (10 μg/mL) and immediately analyzed under a fluorescence microscope to evaluate the percentage of apoptotic segmented nuclei/cells [43].

Animals

For toxicity studies of SFN complexes, female nude mice (age: 6 wk.; $n = 4$ per treatment group) were purchased from Harlan Italy (now Envigo, S. Pietro al Natisone, Italy). All animals were housed in microisolator cages under germ-free conditions and

placed in laminar-flow racks. They received autoclaved food and water. Once arrived, they were allowed a 7 d period before use. Mice were treated for 5 consecutive days (q1–5) with 30 mg/Kg SFN (*os*), and oCyD/SFN and pCyD/SFN (*ip*) and observed daily (for 8 d) for signs of toxicity and survival. SFN was suspended in water with 1% DMSO, while oCyD/SFN and pCyD/SFN solutions were diluted in water, thus containing 0.1% DMSO. Mice were sacrificed with CO_2 on day 8.

All experiments were performed in accordance with the guidelines of the Federation of European Laboratory Animal Science Associations, approved by the Institutional Review Board for animal studies.

Toxicity and histochemical studies

Immediately after the autopsy the fresh kidney, liver and lung tissues were removed and fixed in paraformaldehyde in 0.1 PBS (pH 7.4) for 24 h, processed routinely, embedded in Paraplast (Sigma-Aldrich, Milano, Italy) wax and sectioned at 6 μm. Sections from all organs were then stained with haematoxylin/eosin (H&E) and mounted with DPX for histology (Sigma-Aldrich). Digital pictures of samples were taken with a Canon EOS 1200D camera connected to a Zeiss Axioskop II Plus light microscope to perform a qualitative evaluation of tissue sections.

Results and discussion

Two different nanosystems were assayed as solubilizing agents of the poorly water-soluble drug SFN (Fig. 1). In particular, an EPI cross-linked polymer pCyD (Mw of 92 kDa, 55–58 β-CyD cavities, NP diameter 8.8 nm) and an oligomer oCyD (12 kDa, 7 CyD cavities, NP diameter 3.8 nm) [40] were tested. Both pCyD and oCyD significantly affected SFN solubility (Fig. 2). A clear solution of SFN was obtained in the presence of 10 mg/mL of pCyD or oCyD (Fig. 2, vials 3 and 4). In the presence of β-CyD (Fig. 2, vial 2) a suspension was obtained, as was also the case in SFN alone (Fig. 2, vial 1).

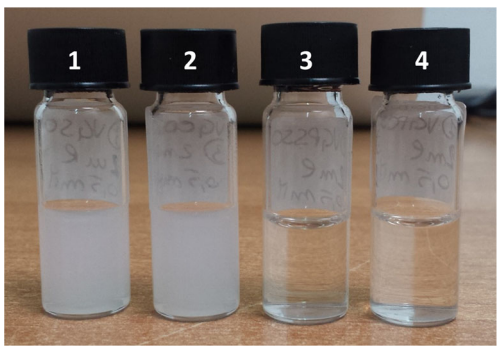

Fig. 2 SFN (0.40 mg/mL) in water alone (1) or with 10 mg/mL of β-CyD (2); pCyD (3); oCyD (4)

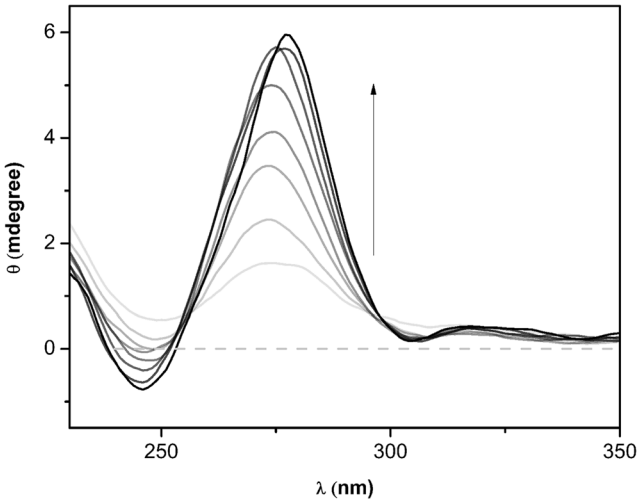

Fig. 3 CD spectra of SFN (read from gray to black: 0.5, 1, 1.5, 2, 2.5, 3, 3.5 & 4 × 10^{-5} M) with oCyD (β-CyD cavity concentration: 1.3 × 10^{-3} M) at pH 7.4 (10 mM Tris buffer)

The inclusion ability of oCyD or pCyD for SFN was investigated using CD spectroscopy. Fig. 3 reports the CD spectra obtained when SFN was added to an oCyD solution at pH 7.4. The spectra show an induced circular dichroism positive band at 275 nm. The intensity of the band increased when the guest/host molar ratio increased, thus suggesting that SFN interacts with the oligomer. The CD spectra of SFN in the presence of pCyD or oCyD is reported in Fig. 4. For a better comparison

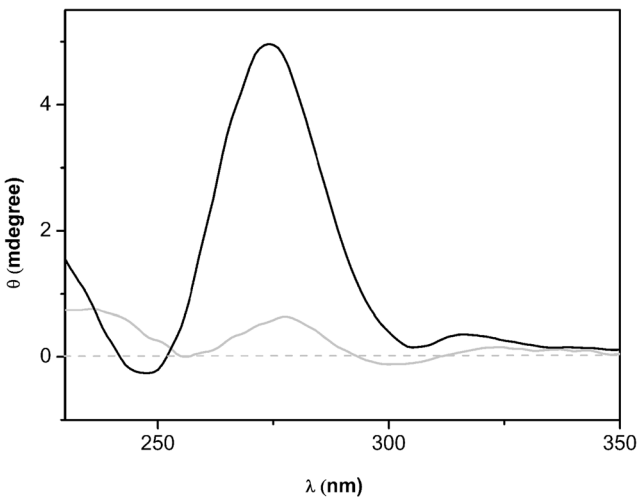

Fig. 4 CD spectra of SFN (2 × 10^{-5} M) with oCyD (black); pCyD (gray); (β-CyD cavity concentration: 1.3 × 10^{-3} M)

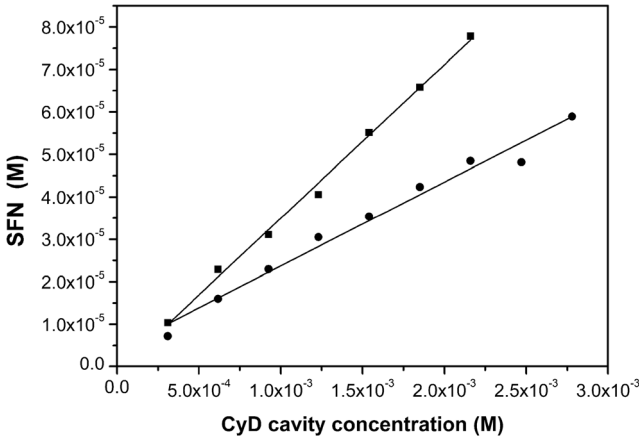

Fig. 5 Solubility of SFN vs. pCyD (●) or oCyD (■) at pH 7.4 (TRIS buffer)

among the hosts, which have a different number of cavities, CD spectra were carried out at the same concentration of CyD cavities in the samples. The highest intensity of the CD bands observed in the case of oCyD may suggest a better interaction of SFN with the CyD units of oCyD. These results are in keeping with the apparent stability constant values discussed below.

Solubility studies

The CE values of polymers with SFN were obtained from solubility measurements using the method described by Higuchi and Connors [41]. This method has been widely used for determining stability constants of drug/CyDs and for polymeric hosts [15, 44–46]. As all the CyD cavities of the polymer were equivalent binding sites, the drug can be included in a single CyD cavity.

The solubility phase diagram, obtained by plotting SFN concentration versus the concentrations of oCyD or pCyD, is reported in Fig. 5. The host concentration is the CyD cavity concentration for a better comparison among the different systems.

We obtained an A_L-type phase diagram with a linear correlation between SFN and the host concentration (slope less of unity). This trend suggests the formation of a 1:1 host/guest inclusion complex with the CyD unit. We found that SFN solubility was not affected by β-CyD in the experimental condition, as reported by others [47]. Interestingly, the solubility of the drug increased linearly with the host (oCyD or pCyD) concentration. The oligomer is more effective than pCyD, and the solubility of SFN in the presence of oCyD significantly increases over 80 μM. This data suggests that a shorter polymer chain shows better solubilizing properties as shown for similar systems [46]. In fact, for polymers with a higher number of CyD units, the cavities become less accessible probably due to steric hindrance.

Loftsson has reported that for poorly water-soluble drugs, the intrinsic solubility (S_0) is in general different from the intercept (S_{int}) value of the phase-solubility diagram, resulting in erroneous $K_{1:1}$ values. Therefore, a preferred parameter for the evaluation of the solubilizing efficiency of CyDs is their CE (i.e. the concentration ratio between complexed and free CyD). It is independent of both S_0 and S_{int}, and more reliable to investigate the influences of different compounds on the solubilization.

CE values for oCyD and pCyD were calculated from the slope of the phase-solubility diagrams (Table 1). The best results were obtained with oCyD. $K_{1:1}$ was also calculated using an S_0 of SFN = 2.1×10^{-8} M [32].

Table 2 IC_{50} values (μM) of SFN and its inclusion complex with pCyD and oCyD

Cellular lines	SFN	pCyD/SFN	oCyD/SFN
MCF-7	8.59 ± 1.17	21.8 ± 3.7	15.9 ± 3.4
HepG2	4.10 ± 0.32	5.99 ± 0.65	7.80 ± 2.34
HGC-27	5.12 ± 1.18	4.24 ± 0.77	2.91 ± 0.39
SKMel-28	8.45 ± 1.07	11.0 ± 1.3	11.2 ± 2.0
K1	12.5 ± 3.2	26.5 ± 3.9	25.1 ± 5.9

All data is the mean (± SD) of 4–7 runs

Antiproliferative activity (MTT assay)

The SFN inclusion complexes pCyD/SFN and oCyD/SFN were evaluated for their antiproliferative effects on the MCF7, HGC-27, HepG2, SKMel-28 and K1 cancer cell lines and compared to SFN. Table 2 reports the IC_{50} values obtained. Interestingly, the administration of SFN included in pCyD and oCyD did not

Table 1 CE and apparent stability constant (K) values for the inclusion of SFN in pCyD and oCyD (25 °C, TRIS buffer pH 7.4)

Host	CE	$K_{1:1}$ (M^{-1})	Slope	S_{int}
pCyD	0.020 ± 0.001	9.5 (±0.5) ×10^5	0.020 ± 0.001	3.4 (±0.9) ×10^{-6}
oCyD	0.035 ± 0.002	1.7 (±0.1) ×10^6	0.034 ± 0.002	7 (±1) ×10^{-7}

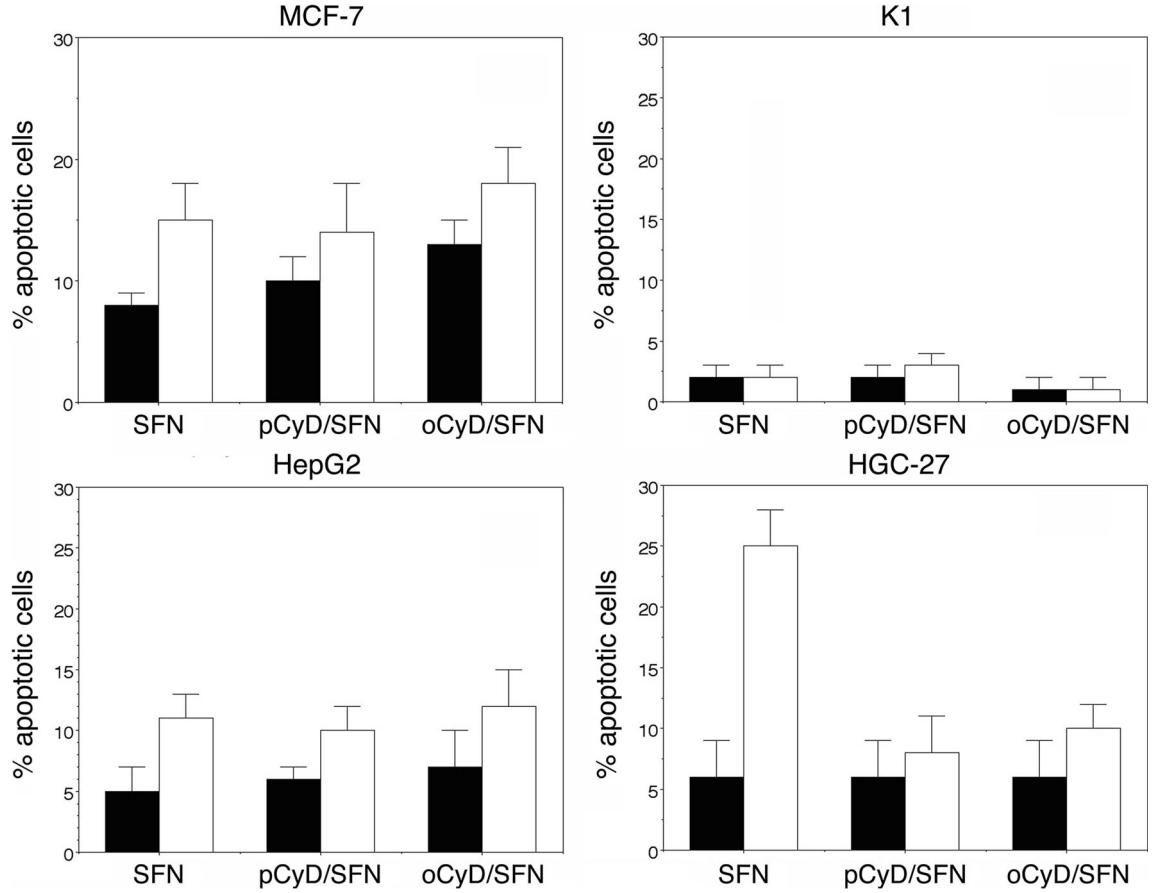

Fig. 6 Apoptotic activity of SFN, pCyD/SFN and oCyD/SFN in four tumor cell lines. Bars represent the mean ± SD of 4–8 data. IC_{50}, (■), IC_{75}, (□)

undergo any significant reduction in its antiproliferative activity in two of the cell lines treated (HepG2 and SKMel-28). In K1 and MCF-7 lines, the polymers decreased the activity of SFN (on average 113 ± 26%), while oCyD seems to improve the activity slightly (+43%) in HGC-27.

The reduced antiproliferative effect of the CyD polymer/SFN complexes in comparison to SFN in some cell lines is in keeping with the trend reported for other drug delivery nanoparticles [48, 49].

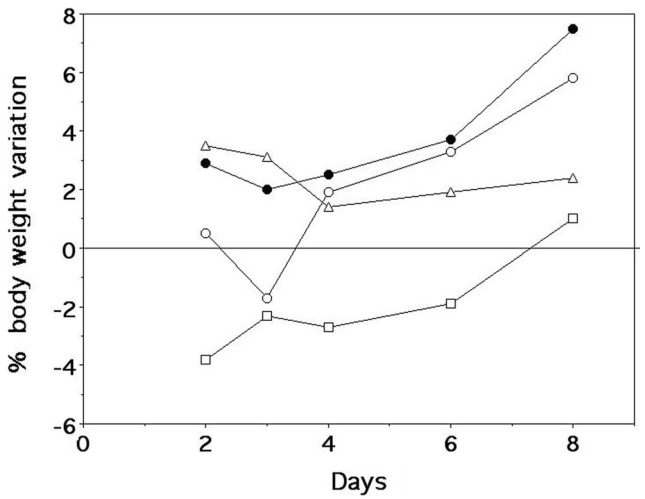

Fig. 7 Percent body weight variation in mice treated with SFN and its complexes. Control (●), SFN (○), pCyD/SFN (□), oCyD/SFN (Δ). SDs were omitted to avoid confusion

Visualization of apoptotic cells/nuclei by DAPI

We tested the ability of SFN, pCyD/SFN and oCyD/SFN to trigger apoptosis in MCF-7, K1, HepG2 and HGC-27 cells through an analysis of the morphology of DAPI stained nuclei and after exposure to equitoxic drug concentrations (IC_{50} and IC_{75}). As shown in Fig. 6, all preparations demonstrated a good level of apoptotic activity in all cell lines with a clear dose-response correlation, except in K1. As for their specific activity, SFN and its complexes showed comparable activities in HepG2, K1 and MCF-7 cells, while SFN was more active than oCyD/SFN and pCyD/SFN in HGC-27 cells.

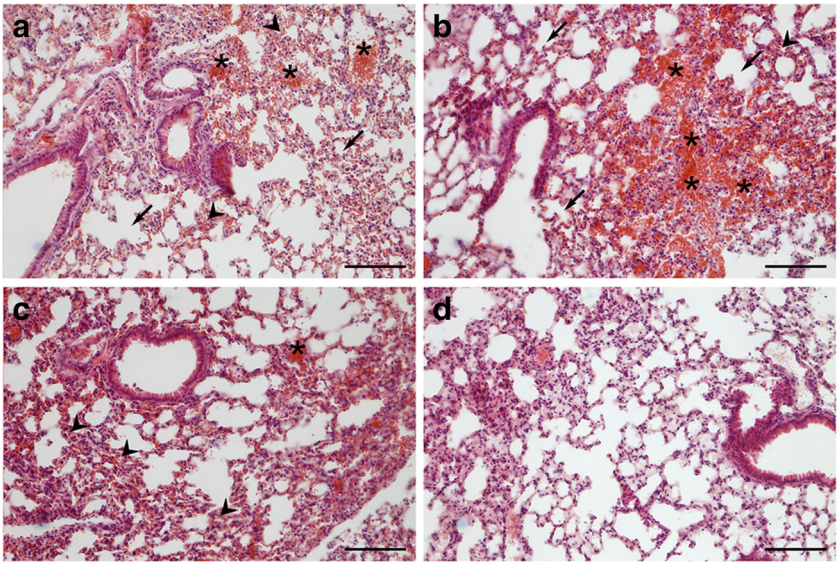

Fig. 8 Lung histology. Panel (**a**), control mice administered with distilled water containing 0.1% DMSO. Panel (**b**), mice treated with SFN per *os* at 30 mg/Kg q1–5. Panels (**c**) and (**d**), animals treated with pCyD/SFN and oCyD/SFN, respectively, at 30 mg/Kg q1–5. Altered alveolar morphology: arrow. Thickened walls: arrowhead. Erythrocyte congestion: asterisk. Scale bar: 100 μm

In vivo experiments

We also determined the in vivo tissue toxicity of a standard dose of SFN (*os*) and its soluble complexes (*ip*, 30 mg/Kg, all given daily for 5 consecutive days). The percentage variation in body weight of treated mice is reported in Fig. 7. In sum, no significant weight variations were observed after the administration of the complex oCyD/SFN. Negative weight variations were observed for SFN (day 3) and pCyD/SFN (from day 2–6), but only for pCyD/SFN these variations were significantly different ($p < 0.02$) than those of control mice.

These results suggest a lower general toxicity for oCyD/SFN as compared to SFN and pCyD/SFN. Treatment with oCyD/SFN causes a significant, although not impressive, loss of weight as compared to control mice.

Histological analysis of the main organs

Morphological analysis of the lung showed a very slight effect of the 0.1% DMSO-containing solvent on lung structure. In fact, we observed some almost normal areas and others with altered alveolar morphology, thickened walls and the presence of erythrocyte congestion (Fig. 8). On the other hand, after SFN administration, we observed more extensively altered parenchymal areas with compromised alveolar morphology, the collapse of the alveolar component and erythrocyte congestion.

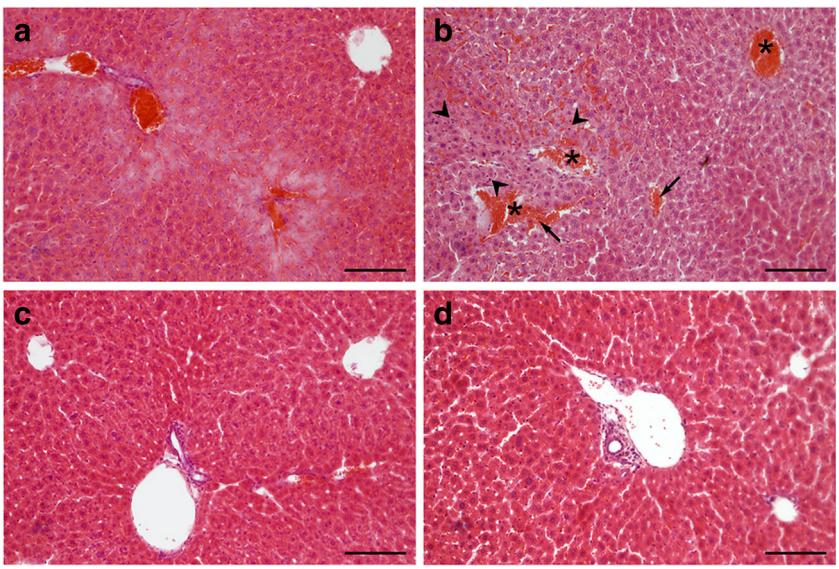

Fig. 9 Liver histology. Panel (**a**), control mice administered with distilled water containing 0.1% DMSO. Panel (**b**), mice treated with SFN per *os* at 30 mg/Kg q1–5. Panels (**c**) and (**d**), animals treated with pCyD/SFN and oCyD/SFN, respectively, at 30 mg/Kg q1–5. Dilated sinusoids: arrow. Vessels congested by erythrocyte: asterisk. Hepatocytes with pycnotic nuclei: arrowhead. Scale bar: 100 μm

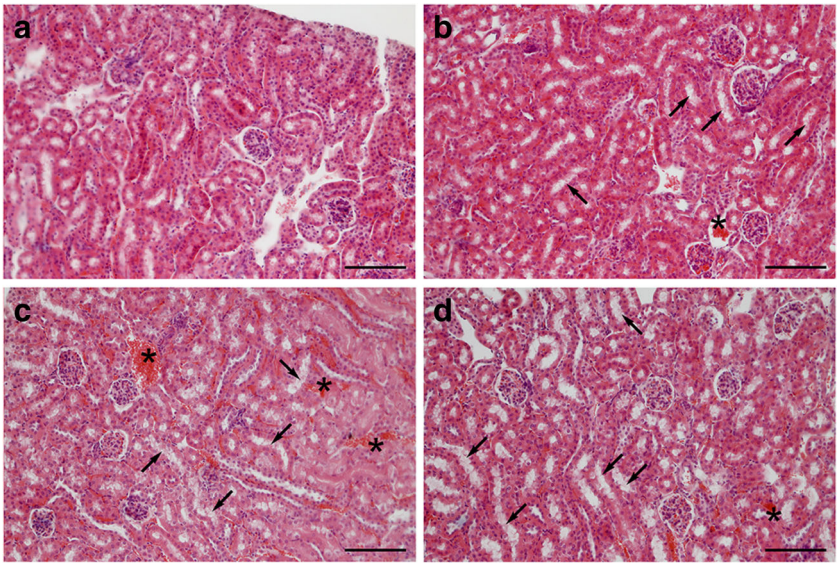

Fig. 10 Kidney histology. Panel (**a**), control mice administered with distilled water containing 0.1% DMSO. Panel (**b**), mice treated with SFN per *os* at 30 mg/Kg q1–5. Panels (**c**) and (**d**), animals treated with pCyD/SFN and oCyD/SFN, respectively, at 30 mg/Kg q1–5. Proximal tubules with fringed epithelium: arrow. Vessels containing congested erythrocytes: asterisk. Scale bar: 100 μm

After *ip* administration of pCyD/SFN, we observed a greater frequency of impaired parenchymal areas, always coupled with a moderate erythrocyte congestion. However, after *ip* treatment with oCyD/SFN, only occasional alterations of parenchyma, accompanied by reduced erythrocyte congestion, were observed.

While analyzing the liver sections in control mice, we observed some very light tissue alterations in the periportal areas. On the contrary, after the administration of SFN (per os), dilated sinusoidal areas, vessels frequently congested by erythrocyte and occasionally amorphous material were evident. In some areas of the section, we also observed the presence of hepatocytes with irregular (pycnotic) nuclei. On the other hand, liver sections of mice treated with pCyD/SFN present sinusoids with a regular appearance and hepatocyte laminae regular in appearance. A similar situation was also observed in animals treated with oCyD/SFN (Fig. 9).

In control kidney sections, the cortical area did not present any evident alterations (Fig. 10). We observed the presence of some proximal tubules with fringed epithelium and occasional vessels containing congested erythrocytes in kidney sections from animals treated with SFN, while we recorded a greater presence of proximal tubules with altered epithelium and vessels congested by erythrocytes in mice treated with pCyD/SFN. After *ip* treatment with oCyD/SFN, the histological situation was similar to what was observed after pCyD/SFN treatment. The medullary area showed no evidence of morphological differences in either treated or control animals.

Conclusions

Cyclodextrin (CyD) nanocarriers were used to efficiently solve the low-solubility issue with sorafenib (SFN). CyD cross-linked polymers with different molecular weights were used to prepare soluble supramolecular complexes with SFN up to 80 μM. The CyD polymer/SFN complexes were able to inhibit cell proliferation and trigger apoptosis in the cell lines used. Our results indicate that CyD polymer/SFN complexes have lower in vivo toxicity than SFN alone. In particular, oCyD/SFN showed the lowest toxicity in the lung, where SFN alone showed a strong toxicity under our experimental conditions. The toxicological data was also confirmed by a lower general toxicity of oCyD/SFN in comparison to SFN or pCyD/SFN. Moreover, both the polymer/SFN complexes showed almost no liver toxicity as compared to SFN. Overall, our results suggest that CyD polymers could provide a new formulation strategy for the delivery of SFN, thus moving to class I (Biopharmaceutics Classification System), in order to increase its bioavailability and reduce its systemic toxicity.

Acknowledgements The authors acknowledge the Consorzio Interuniversitario di Ricerca in Chimica dei Metalli nei Sistemi Biologici (CIRCMSB) and the Italian Ministero dell'Università e della Ricerca.

Funding This study was funded by FIRB RINAME.

Compliance with ethical standards

Conflict of interest All the authors declare that they have no conflict of interest.

Ethical approval All applicable international, national, and/or institutional guidelines for the care and use of animals were followed. This article does not contain any studies with human participants performed by any of the authors.

References

1. Popielec A, Loftsson T (2017) Effects of cyclodextrins on the chemical stability of drugs. Int J Pharm 531:532–542
2. Khan AR, Forgo P, Stine KJ, D'Souza VT (1998) Methods for selective modifications of cyclodextrins. Chem Rev 98:1977–1996
3. Oliveri V, Vecchio G (2016) Cyclodextrins as protective agents of protein aggregation: an overview. Chem Asian J 11:1648–1657
4. Heidel JD, Schluep T (2012) Cyclodextrin-containing polymers: versatile platforms of drug delivery materials. J Drug Deliv ID 262731:17
5. Arima H, Hayashi Y, Higashi T, Motoyama K (2015) Recent advances in cyclodextrin delivery techniques. Expert Opin Drug Deliv 12:1425–1441
6. Giglio V, Oliveri V, Viale M, Gangemi R, Natile G, Intini FP, Vecchio G (2015) Folate–cyclodextrin conjugates as carriers of the platinum(IV) complex LA-12. ChemPlusChem 80:536–543
7. Bellia F, La Mendola D, Pedone C, Rizzarelli E, Saviano M, Vecchio G (2009) Selectively functionalized cyclodextrins and their metal complexes. Chem Soc Rev 38:2756–2781
8. Lakkakula JR, Maçedo Krause RW (2014) A vision for cyclodextrin nanoparticles in drug delivery systems and pharmaceutical applications. Nanomedicine 9:877–894
9. Van de Manakker F, Vermonden T, Van Nostrum CF, Hennink WE (2009) Cyclodextrin-based polymeric materials: synthesis, properties, and pharmaceutical/biomedical applications. Biomacromolecules 10:3157–3175
10. Vulic K, Shoichet MS (2014) Affinity-based drug delivery systems for tissue repair and regeneration. Biomacromolecules 15:3867–3880
11. Jones RK, Caldwell JE, Brull SJ, Soto RG (2008) Reversal of profound rocuronium-induced blockade with sugammadex: a randomized comparison with neostigmine. Anesthesiology 109:816–824
12. Gidwani B, Vyas AA (2015) Comprehensive review on cyclodextrin-based carriers for delivery of chemotherapeutic cytotoxic anticancer drugs. BioMed Res Int 2015. https://doi.org/10.1155/2015/198268
13. Adeoye O, Cabral-Marques H (2017) Cyclodextrin nanosystems in oral drug delivery: a mini review. Int J Pharm doi: https://doi.org/10.1016/j.ijpharm.2017.04.050
14. Avnesh S, Thakor MD, Sanjiv S, Gambhir MD (2013) Nanooncology: the future of cancer diagnosis and therapy. Cancer J Clin 63:395–418
15. Fülöp Z, Kurkov SV, Nielsen TT, Larsen KL, Loftsson T (2012) Self-assembly of cyclodextrins: formation of cyclodextrin polymer-based nanoparticles. J Drug Deliv Sci Technol 22:215–222
16. Oliveri V, Bellia F, Vecchio G (2017) Cyclodextrin nanoparticles bearing 8-hydroxyquinoline ligands as multifunctional biomaterials. Chem Eur J 23:442–4449
17. Swaminathan S, Cavalli R, Trotta F (2016) Cyclodextrin-based nanosponges: a versatile platform for cancer nanotherapeutics development. Wiley Interdiscip Rev Nanomed Nanobiotechnol 8:579–601
18. Zhu W, Li Y, Liu L, Chen Y, Wang C, Xi F (2010) Supramolecular hydrogels from cisplatin-loaded block copolymer nanoparticles and α-Cyclodextrins with a stepwise delivery property. Biomacromolecules 11:3086–3092
19. Oliveri V, Bellia F, Viale M, Maric I, Vecchio G (2017) Linear polymers of β and γ cyclodextrins with a polyglutamic acid backbone as carriers for doxorubicin. Carbohydr Polym. 177:355–360
20. Davis ME, Zuckerman JE, Choi CH, Seligson D, Tolcher A, Alabi CA, Yen Y, Heidel JD, Ribas A (2010) Evidence of RNAi in humans from systemically administered siRNA via targeted nanoparticles. Nature 464:1067–1070
21. Clark AJ, Wiley DT, Zuckerman JE, Webster P, Chao J, Lin J, Yen Y, Davis ME (2016) CRLX101 nanoparticles localize in human tumors and not in adjacent, nonneoplastic tissue after intravenous dosing. PNAS 113:3850–3854
22. Hu C-MJ, Fang RH, Luk BT, Zhang L (2014) Polymeric nanotherapeutics: clinical development and advances in stealth functionalization strategies. Nano 6:65–75
23. Gidwani B, Vyas A (2014) Synthesis, characterization and application of epichlorohydrin-β-cyclodextrin polymer. Colloids Surf B 114:130–137
24. Giglio V, Sgarlata C, Vecchio G (2015) Novel amino-cyclodextrin cross-linked oligomer as efficient carrier for anionic drugs: a spectroscopic and nanocalorimetric investigation. RSC Adv 5:16664–16671
25. Kanwar JR, Long BM, Kanwar RK (2011) The use of cyclodextrins nanoparticles for oral delivery. Curr Med Chem 18:2079–2085
26. Anand R, Malanga M, Manet I, Manoli F, Tuza K, Aykac A, Ladaviere C, Fenyvesi E, Vargas-Berenguel A, Gref R, Monti S (2013) Citric acid-γ-cyclodextrin crosslinked oligomers as carriers for doxorubicin delivery. Photochem Photobiol Sci 12:1841–1854
27. Folch-Cano C, Yazdani-Pedram M, Olea-Azar C (2014) Inclusion and functionalization of polymers with cyclodextrins: current applications and future prospects. Molecules 19:14066–14079
28. Sherje AP, Dravyakar BR, Kadam D, Jadhav M (2017) Cyclodextrin-based nanosponges: a critical review. Carbohydr Polym 173:37–49
29. Longmire M, Choyke PL, Kobayashi H (2008) Clearance properties of nano-sized particles and molecules as imaging agents: considerations and caveats. Nanomedicine (London) 3:703–717
30. Huillard O, Boissier E, Blanchet B, Thomas-Schoemann A, Cessot A, Boudou-Rouquette P, Durand JP, Coriat R, Giroux J, Alexandre J, Vidal M, Goldwasser F (2014) Drug safety evaluation of sorafenib for treatment of solid tumors: consequences for the risk assessment and management of cancer patients. Expert Opin Drug Saf 13:663–673
31. European Medicines Agency. Sorafenib—EPAR Scientific Discussion (2010)
32. Almeida e Sousa L, Reutzel-Edens SM, Stephenson GA, Taylor LS (2015) Assessment of the amorphous "solubility" of a Group of Diverse Drugs Using new Experimental and Theoretical Approaches. Mol. Pharmaceutics 12:484–−495
33. Liu C, Chen Z, Chen Y, Lu J, Li Y, Wang S, Wu G, Qian F (2016) Improving oral bioavailability of Sorafenib by optimizing the "spring" and "parachute" based on molecular interaction mechanisms. Mol Pharm 13:599–608
34. Bondì ML, Scala A, Sortino G, Amore E, Botto C, Azzolina A, Balasus D, Cervello M, Mazzaglia A (2015) Nanoassemblies based on supramolecular complexes of nonionic amphiphilic cyclodextrin and sorafenib as effective weapons to kill human HCC cells. Biomacromolecules 16:3784–3791
35. Zhang N, Zhang B, Gong X, Wang T, Liu Y, Yang S (2016) In vivo biodistribution, biocompatibility, and efficacy of sorafenib-loaded lipid-based nanosuspensions evaluated experimentally in cancer. Int J Nanomedicine 11:2329–2343
36. Blanchet B, Billemont B, Barete S, Garrigue H, Cabanes L, Coriat R, Francès C, Knebelmann B, Goldwasser F (2010) Toxicity of sorafenib: clinical and molecular aspects. Expert Opin Drug Saf 9:275–287
37. Yamaguchi T, Seki T, Miyasaka C, Inokuchi R, Kawamura R, Sakaguchi Y, Murata M, Matsuzaki K, Nakano Y, Uemura Y, Okazaki K (2015) Interstitial pneumonia induced by sorafenib in a patient with hepatocellular carcinoma: an autopsy case report. Oncol Lett 9:1633–1636
38. Van Hootegem A, Verslype C, Van Steenbergen W (2011) Sorafenib-induced liver failure: a case report and review of the

Literature. Case Reports in Hepatology. http://dx.doi.org/10.1155/2011/941395

39. Guo Y, Zhong T, Duan X-C, Zhang S, Yao X, Yin Y-F, Huang D, Ren W, Zhang Q, Zhang X (2017) Improving anti-tumor activity of sorafenib tosylate by lipid- and polymer-coated nanomatrix. Drug Deliv 24:270–277
40. Giglio V, Viale M, Monticone M, Aura AM, Spoto G, Natile G, Intini FP, Vecchio G (2016) Cyclodextrin polymers as carriers for the platinum-based anticancer agent LA-12. RSC Adv 6:12461–12466
41. Loftsson T, Hreinsdottir D, Masson M (2005) Evaluation of cyclodextrin solubilization of drugs. Int J Pharm 302:18–28
42. Oliveri V, Puglisi A, Viale M, Aiello C, Vecchio G, Clarke J, Milton J, Spencer J (2013) New cyclodextrin-bearing 8-hydroxyquinoline ligands as multifunctional molecules. Chem Eur J 19:13946–13955
43. Mariggiò MA, Cafaggi S, Ottone M, Parodi B, Vannozzi MO, Parodi A, Mandys V, Viale M (2004) Inhibition of cell growth: induction of apoptosis and mechanism of action of the novel platinum compound cis-diaminechloro-[2-(diethylamino) ethyl 4- amino-benzoate, N4]-chloride platinum (II) monohydrochloride monohydrate. Invest New Drugs 22:3–16
44. Layre AM, Gosselet NM, Renard E, Sebille B, Amiel C (2003) Comparison of the complexation of cosmetic and pharmaceutical compounds with β-cyclodextrin, 2-hydroxypropyl-β-cyclodextrin and water-soluble-β-cyclodextrin-co-epichlorohydrin polymers. J. Inclusion Phenomen Macrocyclic Chem 43:311–317
45. Martin R, Sánchez I, Cao R, Rieumont J (2006) Solubility and kinetic release studies of naproxen and ibuprofen in soluble Epichlorohydrin-β-cyclodextrin polymer. Supramol Chem 18:627–631
46. Fülöp Z, Nielsen TT, Larsen KL, Loftsson T (2013) Dextran-based cyclodextrin polymers: their solubilizing effect and self-association. Carbohydr Polym 97:635–642
47. Hashemi F, Tamaddon AM, Yousefi GH, Farvadi F (2012) Effect of pH on Solubilisation of Practically Insoluble Sorafenib by Classic and Stealth Polyamidoamine (PAMAM) Dendrimers and β–cyclodextrin. Proc NAP 1:02NNBM06
48. Haxton KJ, Burt HM (2009) Polymeric drug delivery of platinum based anticancer agents. J Pharm Sci 98:2299–2316
49. Viale M, Rossi M, Russo E, Cilli M, Aprile A, Profumo A, Santi P, Fenoglio C, Cafaggi S, Rocco M (2015) Fibrin gels loaded with cisplatin and cisplatin-hyaluronate complexes tested in a subcutaneous human melanoma model. Invest New Drugs 33:1151–1161